A Novel Level Set Image Segmentation Approach with Autonomous Initialization Contour

Xiaowei He, Zhuan Song and Junli Fan

College of Mathematics, Physics and Information Engineering, Zhejiang Normal University, Jinhua 321004, China
jhhxw@zjnu.cn, shmx_624@163.com, fjl9008@163.com

Abstract

The image segmentation result based on level set typically depends on the appropriate manual initial contour. In this paper, we introduce an autonomous approach for deciding the initial level set contour to be close to the actual boundary as far as possible, and the decided initial contour can be directly evolved by various level set methods. Such an improvement can speed up the evolution and lead to a more robust segmentation result. Then, we consider the statistical information of three distinct regions to construct a new level set model, including contour, contour inside and outside. Combining the two steps above is helpful to obtain a pretty ideal segmentation effect. Some remarkable results and shorter execution time for some difficult segmentation tasks shown in this paper demonstrate the potential of our innovative approach.

***Keywords**: Image Segmentation, Level Set, Autonomous Initial Contour, Curve Evolution*

1. Introduction

Image segmentation is a technique for partitioning an image into uniform and non-overlapping regions based on some similar measure[3]. It has been used in the fields including computer vision, image analysis, medical image processing, remote sensing, geographical information and so on. To partition different kinds of images perfectly, many segmentation approaches have been proposed in past decades. In recent years, active contour model has also become an important method for image segmentation task. Active contour model (also named Snake model) was first proposed in [7], which is a minimization problem for the energy guided by external constraint forces and influenced by image forces that pull it toward lines and edges. The main features of this method are its ability of efficiently integrating low-level visual characteristics of an image with human prior knowledge [7, 8]. But it has no ability to achieve a good result when the topological structure of the evolution curves changes. Shortly afterwards, the level set method for capturing moving fronts was introduced in [15], which uses an implicit representation of the interface by embedding it into a domain of one higher-dimension level set function. Level set has been found that it is a robust method for image segmentation. Here we briefly introduce two most frequent types of level set based image segmentation: edge-based and region-based.

Edge-based level set models mainly utilize local information of an image to identify object boundaries [1, 7, 9, 18]. The representative of this type is the geometric active contour(GAC) model[18]. Recently, several edge-based level set models are proposed for various targets. A gradient-based approach was proposed to perform 2D and 3D deformable model segmentation using level set[11]. A level set evolution method is implemented on the feature image obtained by convolving the data-adaptive Gaussian smoother with the original image instead of classical Gaussian filter[14],which has advantages in extracting contours of the noise and weak contrast image and level set evolution speed. Generally, the evolution of these methods is typically based on the edges and plane curves, and one benefit of them is that no global information of the image is needed. However, edge-based level set models have been found to be very sensitive to image noise and highly dependent on the position of the initial contour.

Another type of level set segmentation methods is always based on regional information of an image and have been focused on in past decade [5, 12, 17]. One of the most famous and widely used region-based level set method is the active contour without edge model (also named C-V model) [17]. Chan and Vese proposed this model using the region information of an image rather than the gradients on the boundaries. Recently, a geometric active contour model in a partial differential equation formulation is proposed in [4], which is directly derived from the mean curvature motion with a transition region-based external force. To reduce the impact of intensity inhomogeneity to image segmentation, a region-based level set (RBLS) model was proposed in [19]. The proposed model utilizes both global image information and local image information.

Comparatively speaking, region-based level set methods have many advantages over those edge-based methods. First, they use the statistical information internal and external areas of the contour to control the evolution, which is less sensitive to noises, and at final, they probably obtain better effect for those images with weak edges or without edges. Second, they are also less sensitive to the position of the initial contour, and usually can efficiently detect the exterior and interior boundaries simultaneously[6]. Thus, though the foreground and background may be heterogeneous in some images, correct segmentation results can still be achieved [12]. In this paper, we pay more attention to the region-based level set method and we review three different region-based level set methods which our approach is relevant to.

C-V method [17] is the most famous region-based approach which is based on the total squared difference of intensities of those points inside and outside of the contour. Therefore, it is obviously a global-information based method and still works well for the inhomogeneous image. Even if the image is very noisy, the boundaries are always easily detected by it. However, C-V model similarly also has the disadvantages as following. Firstly, it is undoubtedly influenced by the initial position of the contour and then it always falls into a local solution by an improper initialization. As a result, some complicated images cannot be segmented out successfully by one simple initial contour or an improper initial position. A different formulation was proposed where the implicit function is modeled as a continuous parametric function expressed on a B-spline basis [10]. In this model, the evolving interface $\Gamma \subset \mathbb{R}^{d}$ is represented by the zero level-set of an implicit function $\phi(\cdot)$ expressed as a linear combination of B-spline basis functions. Another region-based ACM[6], which is implemented with a special processing named Selective Binary and Gaussian Filtering Regularized Level Set (SBGFRLS) was proposed. The authors utilize the statistical information inside and outside the contour to construct a region-based signed pressure force (SPF) function instead of an edge function [2], which is able to control the direction of evolution. This method combines the merits of the traditional GAC and C-V models, which possess the advantages of regional and global segmentation methods. By this way, it can reduce the expensive re-initialization of the traditional level set method and it becomes more efficient. But we can still see the two methods above are unable to segment those especially blurry and complicated images (see Section 4).

These three region-based level set models above all need manual initialization in advance for deciding the zero level set, by which the entire image is divided into two regions of an interior and exterior of the contour. Then the interior mean and the exterior mean are used to construct an evolutionary function. However, these methods have not considered the contribution of the zero level set itself, which is usually very important for some blurry images. In this paper, our main contributions include the following two items. Firstly, we introduce an autonomous region-based approach for deciding an initial level set contour instead of manual contour. The decided initial contour is always very close to the actual contours of objects and can be directly evolved instead of artificial positioning. Secondly, we also propose a novel level set method, which utilizes three regions intensities means to construct an evolutionary function. By adding the intensities mean of the neighboring area of the contour, blurry regions of objects can be segmented out better. A series of experiments here demonstrate that the combination of the autonomous initialization and the novel level set not only can extract the desired edges of objects but also cost relatively fewer iterations and spend computation time, especially for complicated segmentation tasks.

The remainder of this paper is organized as follows. In Section 2, we propose a new method and some implementation details for it . Then, we corroborate the effectiveness of our proposed method by comparing with various methods with various obscure images and give relevant discussion in Section 3. At last section, we make a conclusion and give some preliminary ideas for future research in this field.

2. The Proposed Method

In this section, we introduce our approach by details. In Subsection 2.1, the novel autonomous initialization method is firstly introduced. Then, we give a new level set evolution model based on three regions statistical information in Subsection 2.2. In Subsection 2.3, we give the algorithm combining the two steps above.

2.1. An Autonomous Approach for Deciding Initial Contour

The following four formulas are designed for obtaining the initial contour for level set segmentation approach. (2.1) and (2.2) are used to initialize zero level set $\phi(t=0)$, and formula (2.3) and (2.4) are used for adjusting it before partitioning actual image.

(mean intensity c) $$c = \int_\Omega I(x)dx \,/ \int_\Omega dx, \tag{2.1}$$

(intensity difference $doi\ (x)$) $$doi\ (x) = \frac{I(x)\text{-}c}{\left|\max\left(I(x)\text{-}c\right)\right|}, \tag{2.2}$$

(zero level set ϕ_0^δ) $$\phi_0^\delta = \{x \| doi(x)| < \delta\}, \delta > 0, \tag{2.3}$$

(adjusting ϕ_0^δ) $$\phi^\delta(x, t=0) = \{x \| \lambda_0 \cdot doi(x) - \alpha_0| < \delta\}, \lambda_0, \delta > 0, \tag{2.4}$$

Where Ω :whole image; $I(x)$:the intensity for the point x; c :mean intensity of whole image; $doi\ (x)$: intensity difference between point x and c, λ_0 , α_0, δ : constants for adjusting.

c in (2.1) is a constant of intensity representing the mean intensity of entire image and it meets $Min(I(x)) < c < Max(I(x))$. Here, we adopt doi to indicate the normalization value for the intensity difference between every point in the image and the mean value of c. According to (2.2), the sign of $doi(x)$ for larger intensity point ($I(x) > c$) is positive, and the sign of it for smaller intensity point ($I(x) < c$) is negative. Then, the image is divided into three parts according to the value of $doi(x)$ for every point, the area inside of curve Γ, the area outside of Γ and Γ itself. Zero level set Γ is usually decided by (2.3) in some actual applications.

Actually, c in (2.1) can be considered as a threshold for deciding the points of the curve Γ inside or outside. But the mean of whole image isn't always the accurate threshold value and ϕ_0^δ may not be the applicative zero level set when the image is heterogeneous or noisy. There may be some positive-value points in the negative region or some negative-value points in the positive region (see Figure1 (a) and (c)). Therefore, we introduce two special constants λ_0 and α_0 in (2.4) to handle reasonably. According to the intensities information of the image shown in Figure 1 (a), the signs for those noisy or heterogeneous points are same as that of those points of objects, but the $doi(x)$ value of the former are usually near zero and smaller than that of the later. To separate those noisy or heterogeneous points from the points of objects, we multiply doi by a parameter λ_0 to expand its value and to make those noisy or heterogeneous points meet $\lambda_0 \cdot doi(x) - \alpha_0 < 0$, and then they can be regarded as the background points as expected. Therefore, calculating $\lambda_0 \cdot doi\text{-}\alpha_0$ can correct signs of noise or heterogeneous points and classify them into those normal background points near them in image shown in Figure 1 (b). We set $\phi^\delta(x,t=0)$ in (2.4) as the final result of zero level set. Vice versa, by setting different parameters λ_0 and α_0, Figure 1 (c) can be handled and a good effect can be obtained at final (Figure 1 (d)).

It is necessary to explain more details here. Take the two-object image in the Figure 1(a) and (b) as an example, we take parameters $\lambda_0 = 4$ and $\alpha_0 = 1$ respectively. In fact, the intensities of those points in the objects is larger than the mean value c. Hence, any point x among them meets $0 \le doi(x) \le 1$. Intuitively, the intensities of those points in the background should have been smaller than c, that is to say, for any point x in the background should meet $-1 \le doi \le 0$. But the intensities of some noisy points in the background is slightly larger than c but quite smaller than the values of doi for those points in the two objects. Thus, the zero level set obtained by (2.3) can be seen in the Figure 1 (a). According to the method last paragraph (see (2.4)), we use $4 \cdot doi$ to adjust the doi values for noisy points to meet $0 \le 4 \cdot doi \le 1$ all the same, while the doi values of the points of objects are adjusted to meet $4 \cdot doi > 1$. By calculating the values of the expression $4 \cdot doi\text{-}1$, we can find that the values of it for objects points are still larger than 0, while the values for noisy points become smaller than 0 as same as that for ordinary background points. In this way, the values of the expression $4 \cdot doi\text{-}1$ for most background points meet $\phi<0$ and for most object points meet $\phi>0$, then the zero level set can be obtained subsequently as shown in the Figure 1 (b).

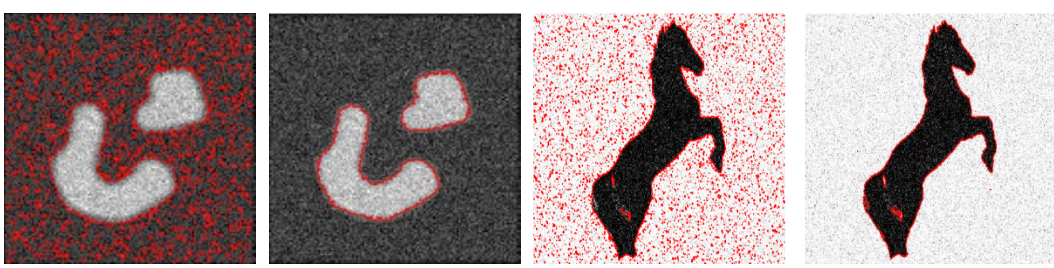

(a) (b) (c) (d)

Figure 1. Initialization of Two Examples. (a) and (b): the Different Initialization Results of Two-objects Image by Expression (2.3) and (2.4), Meeting $I_o > I_b$ and $\alpha_0 > 0$. (c) and (d): the Different Initialization Results of Horse Image by (2.3) and (2.4), meeting $I_b > I_o$ and $\alpha_0 < 0$

How to give the values of constants λ_0 and α_0 can be explained as follows. Actually, the value of α_0 can be positive or negative. There usually exist much more interference factors in the background region than in object regions, such as noise, and usually, heterogeneous part of object regions should be segmented out rather than noise. When the mean intensities of object I_o and that of background I_b meets $I_o > I_b$, α_0 is always taken positive. Otherwise, if $I_o < I_b$, α_0 is always taken negative.

λ_0 is always taken positive in any case. When α_0 has been fixed, λ_0 determines the region size of segmentation object. Here, we simply introduce how to take λ_0 under the situation of $I_o > I_b$, and it is similar for $I_o < I_b$. In the situation of $I_o > I_b$, when λ_0 is taken smaller, then the number of regional points with $\phi>0$ decreases greatly after adjusting by $\lambda_0 \cdot doi$ subtracting α_0, namely the region size of the segmentation object is narrowing more due to the operation of adjusting. Inversely, when λ_0 is taken larger, then after adjusting by $\lambda_0 \cdot doi$ subtracting α_0, the number of regional points with $\phi>0$ reduces marginally, namely the region size of the segmentation object is rarely changed. In some special circumstances, for example, there are some quite blurry parts or the intensities of some parts in the object region very close to those background parts, no matter how large λ_0 is taken, those points in these parts always meet $\lambda_0 \cdot doi < \alpha_0$ and are assigned to the background region by mistake. Under this situation, we can initialize zero level set in the opposite way through taking α_0 as negative. Factly, in this approach , background region is considered as an object to be initialized (an example showns in Figure 2). The above discussion is also suitable for the case of $I_o < I_b$.

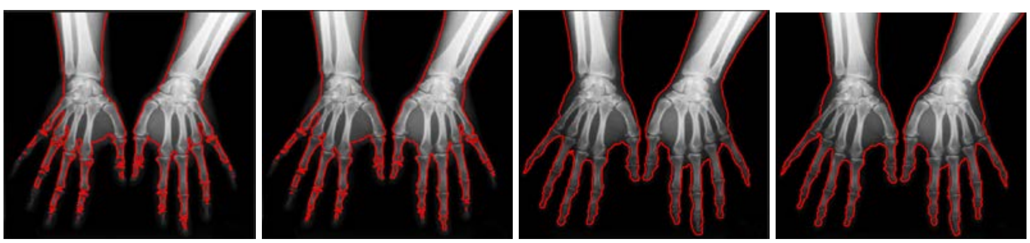

(a) $\alpha_0 = 1$ and $\lambda_0 = 25$ (b) $\alpha_0 = 1$ and $\lambda_0 = 150$ (c) $\alpha_0 = -1$ and $\lambda_0 = 8$ (d) $\alpha_0 = -1$ and $\lambda_0 = 10$

Figure 2. Initialization of Arms-X-ray Image with Different Parameters

Obviously, the image in Figure 2 meets $I_o > I_b$ and α_0 should have be taken positive, but the heads of fingers are too blurry and the intensities of them are very small. We can just obtain the defective initialization results shown in Figure 2 (a) and (b). In order to get better initialization result, we take the background as the segmented object instead of two visual white hands and set α_0 be negative. Then, better initialization results in Figure 2(c) and (d) are achieved.

2.2. Level Set Evolution Model

In this subsection, we give our novel level set model based on regional intensity information. Our method is formulated by minimizing an intensity-based energy function. The basic idea of the model is to constantly adjust constant intensity means c_i of the contour itself, contour inside and outside and then the function reaches its minimum. We construct a function $dori$ (the difference of regions intensity) as follows:

$$dori = (I\text{-}c_0) + (I\text{-}c_1) + (I\text{-}c_2), \tag{2.5}$$

Where c_0, c_1 and c_2 are the constant intensity means of the contour, contour inside and outside respectively.

During each iterative, the last iteration result ϕ is fixed, then c_0, c_1 and c_2 are defined as follows:

$$c_i = \frac{\iint_{\Omega_i} I dxdy}{\iint_{\Omega_i} dxdy}, \ i = 0,1,2, \tag{2.6}$$

Ω_i is a partial region of Ω and changes constantly with the evolution of level set, and its area can be defined depending on the distance to curve Γ. Because ϕ is a constant during each iterative, we calculate its SDF and denote it as ϕ', then Ω_i can be defined as follows:

$$\begin{cases} \Omega_0 = \{x \in \Omega \mid -\delta \le \phi'(x) \le \delta\} \\ \Omega_1 = \{x \in \Omega \mid \ \phi'(x) > \delta\} \\ \Omega_2 = \{x \in \Omega \mid \ \phi'(x) < -\delta\} \end{cases}, \tag{2.7}$$

Where δ is a small positive constant.

The gradient descent flow equation is given as follows:

$$\frac{\partial \phi}{\partial t} = \lambda \cdot \frac{dori}{\max(|dori|)} |\nabla \phi|, \tag{2.8}$$

The value of special parameter λ decides the speed of curve evolution. The smaller λ is set, the slower the speed of evolution is.

A example of Spiral image in Figure 3 shows the validity of our evolution method with ordinary manual initialization. We can see from Figure 3 (d), two perfect results for the two examples are both obtained.

2.3. Implement

In the traditional level set methods, initial contour is always given manually and level set function is initialized to be an SDF to its interface, and re-initialization is required during the evolution processing. In this way, not only the initial contour is not good enough probably, but evolution process always costs more time.

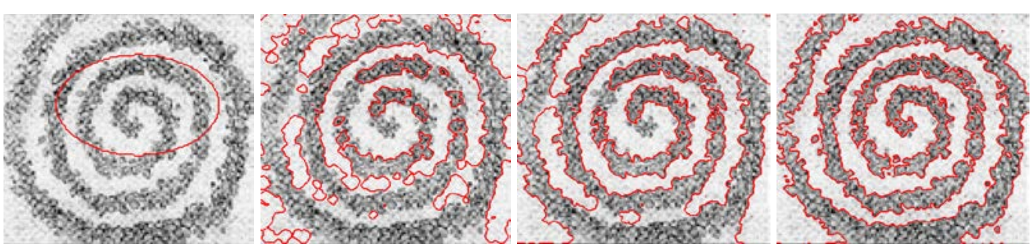

Figure 3. Segmentation Process of Spiral Image by our Method with Manual Initialization. (a): Initial Contours by Manual; the First Row: Revolution from (a) to (d) After 71 Iterations by 3.44s of Whole Calculation Time

Combining our initialization method in Subsection 2.1 and the novel level set model presented in Section 2.2, the main segmentation algorithm is given as follows:

Step1: Using global statistical information, the mean intensity c of image I and doi can be gotten (formula (2.1) and (2.2)).

Step2: According to image information, the parameter λ_0 and α_0 are set to initialize the zero level set by formula (2.4).

Step3: Calculating SDF: Where $\phi > 0$, we set ϕ' as 1; where $\phi < 0$, we set ϕ' as -1.

Step4: Resetting ϕ' with the SDF of ϕ', and saving to get Ω_0, Ω_1 and Ω_2 by (2.7).

Step 5: Do the following steps to evolve the level set function according to (2.8).
Calculate $dori$ (3.5) by c_0, c_1 and c_2 respectively by (2.6);Set parameter λ, compute evolution equation of (2.8);Set integral step dt which meets CFL condition;Compute ϕ^{n+1} by the (2.8) and ϕ^n.

Step6: According to ϕ, we can obtain the boundaries $\partial\Omega$ (where $\phi = 0$) of object, and output the contour C.

Step7: Estimate whether content convergence condition, if not return to step 3.

3. Experiment Results

In contrast to other level set methods, our method utilizes image statistical information to initialize zero level set instead of manual initialization. Our method can efficiently segment images with weak edges or concave edges. Furthermore, our method can also find the interior edges of the objects. In order to demonstrate the strengths of the proposed method, we conclude in this paper by presenting the image segmentation process and results for various images. In particular, every experiment for different approach takes the best or most memorable result and relevant initial contour here. All experiments results confirm that our method has significant good segmentation ability. All algorithms are implemented under a software framework named creaseg [16] with Matlab R2009a in a Windows XP system (Microsoft). All experiments are run on a Lenovo computer with Pentium T2330 CPU 1.60GHz and 1GB RAM.

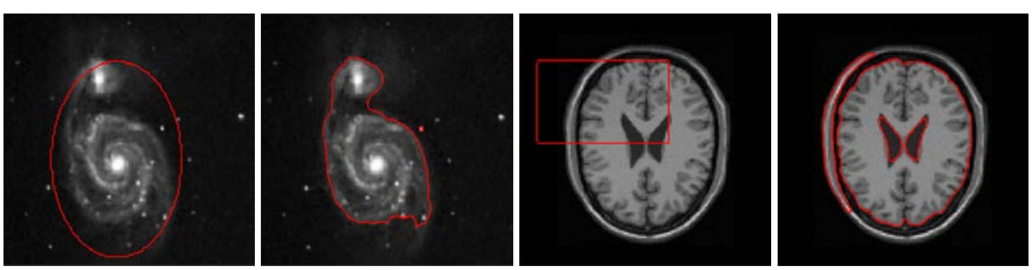

(a1) (b1) (a2) (b2)

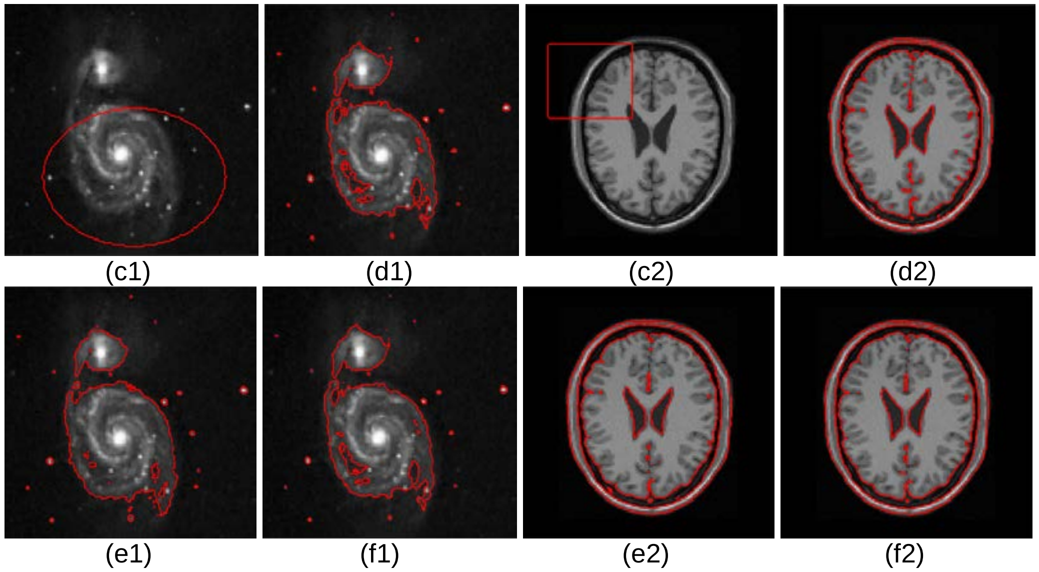

Figure 4. Comparation between CV and ours for Satellite Cloud Image and Brain-MRI image. (a1) and (a2): the initial contours by manual for C-V; (b1) and (b2): the final results by C-V after 261 iterations by 4.16s and after 201 iterations by 2.99s; (c1) and (c2): the initial contours by manual for ours; (d1) and (d2): the final segmentation results by ours respectively after 73 iterations by 1.38s and after 54 iterations by 0.98s; (e1) and (e2): our autonomous contours; (f1): the segmentation result by ours based on (e1) after 12 iterations by 0.44s (include initialization), with $\alpha_0=1, \lambda_0=15$ and $\lambda=25$ **; (f2): the segmentation result by ours based on (e2) after 9 iterations by 0.39s (include initialization), with** $\alpha_0=1, \lambda_0=8$ and $\lambda=5$

Figure 4 shows the segmentation results of the satellite cloud image and the Brain-MRI image with the CV method and our proposed method. The segmentation tasks are difficult because of the weak and irregular boundaries. (a1), (c1), (a2) and (c2) show the initial contours by manual. From (b1) and (b2), they are quite defective with many iterations and more time. (d1) and (d2) show the segmentation results of our method by manual initial contours of (c1) and (c2). Althogh iteration times and calculation time are both less than CV method, they still need many iterations before stopping evolution. In the final row, we give the segmentation results after combining the proposed autonomous initialization and our level set method. (e1) and (e2) show respectively the autonomous initial contours. As we can see, they are very close to the object and provide the very good foundation for the subsequent evolution. Then, (f1) and (f2) show that our segmentation method has better performance with fewer iterations and calculation time.

In Figure 5, our method and Variational B-Spline level set method are compared by applying them to the Eagles image. (a) and (c) show the manual comparatively preferable initial contours. As shown in (b), Variational B-Spline level set method needs fewer iterations and not too much time, but it is fail to segment out the concave region such as the wing of eagle. (d) shows the segmentation result by our method based on manual initialization shown in (c). (e) shows our autonomous initialization contour. (d) and (f) show that an ideal segmentation results can be both obtained, obviously fewer iterations and calculation time are needed by the autonomous initialization method in (f).

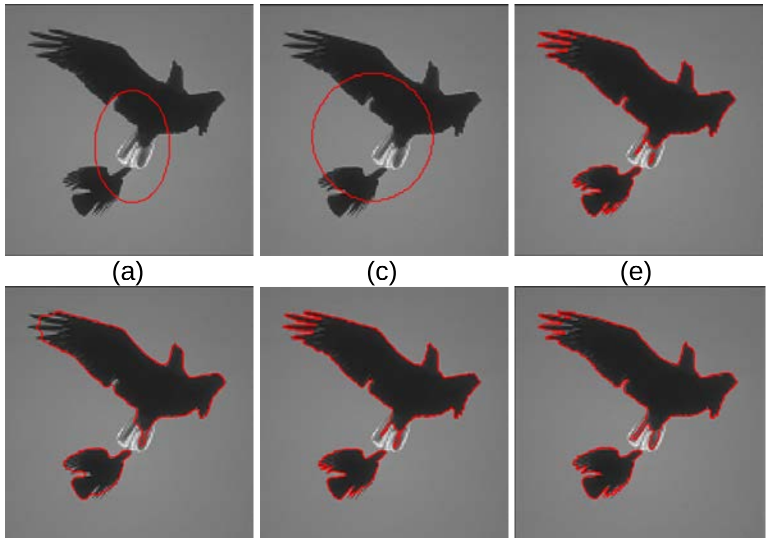

(a) (c) (e)

(b) (d) (f)

Figure 5. Comapration between Bermrd and ours for Eagles Image. (a): the Initial Contour by Manual for Bernard; (b): the Final Deficient or Unsuccessful Segmentation Result by Bernard Method after 11 Iterations by 1.72s; (c): the Initial Contour by Manual for ours; (d): the Final Segmentation Result by ours after 55 Iterations by 0.94s; (e): our Autonomous Contour; (f): the Segmentation Result by ours based on (e) After 16 Iterations by 0.36s (include Initialization), with $\alpha_0 = -1, \lambda_0 = 8$ and $\lambda = 30$

Figure 6 shows the comparison between our method and the SBGFRLS method by applying them to an airplane image. Obviously, the airplane image is also difficult to be segmented for the glaring sun. (a) and (c) show the manual contours around the object. (b) shows the segmentation result of SBGFRLS method based on (a). The contour is far from the object, and the region in the top right corner is easy to be classified together with the object and the curve stops in the wrong place. However, a perfect segmentation result shown in (d) can still be obtained based on (c) by our method. (e) further shows a autonomous good initial contour and we only need to turn the initial contour slightly with our method and then get a perfect result shown in (f).

(a) (c) (e)

(b) (d) (f)

Figure 6. Comparation between SBGFLS and ours for the Airplane Image. (a): the Initial Contour by Manual for SBGFRLS; (b): the Final Unsuccessful Segmentation result after 76 Iterations with SBGFRLS by 0.79s; (c): the Initial Contour by Manual for ours; (d): the Final Segmentation Result by ours after 20 Iterations by 0.47s; (e): our Autonomous Contour; (f): the Segmentation Result by ours based on (e) After 6 Iterations by 0.19s (include initialization), with $\alpha_0 = -1, \lambda_0 = 5$ and $\lambda = 5$

Figure 7 shows the comparative results of a Brain-MRI image with CV, Bernard, SBGFRLS method and our proposed method. According to the experiments, the segmentation task of Brain-MRI image is too difficult to perfectly segment out. In (a), (d) and (g), we give three suitable manual initialization contours respectively, which can help every method to obtain a better result as far as possible. Howerer, the entire object can't be segmented out completely by these three methods, and corresponding best results by them are all not ideal (see (c),(f) and (i)). By the way, we have combined CV, Bernard and SBGFRLS with our autonomous initialization in the experiments not shown here, and the results are all defective almost as same as (c),(f) and (i). (l) shows the effective segmentation consequences of our proposed method with manual initialization. With the autonomous contour showed in (m), obviously, the initialization contour is relatively close to the object and (p) shows that the novel segmentation method has comparatively better performance and costs less calculation time by combining autonomous initial contour.

All these images above are respectively with the feature of weak and irregular boundaries, blurry edges, shadowy interference or heterogeneous intensities. Comparing with C-V model [17], Bernard method [10] and SBGFRLS [6] in the experiments, our proposed method performs more robust and perfect.

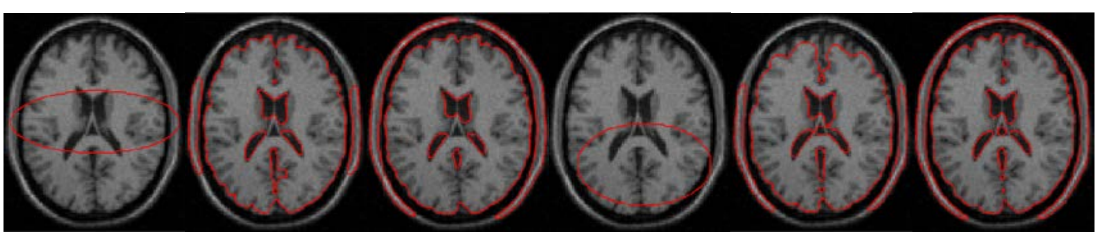

CV:(a) IC (b) 150its (c) 488its Bernard: (d) IC (e) 5 its (f) 22 its

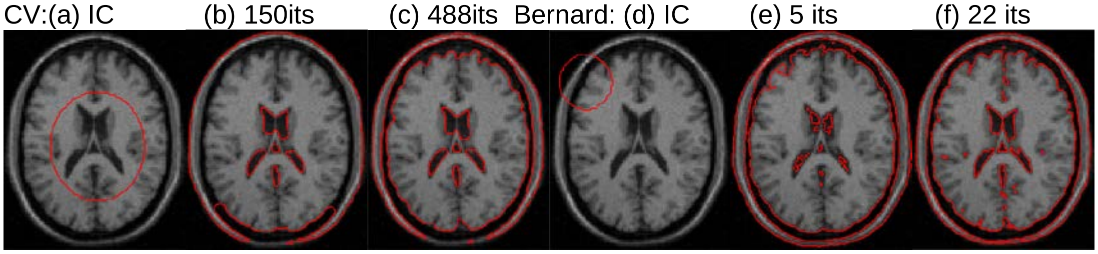

SBGFRLS:(g) IC (h) 15its (i) 70its Ours: (j)IC (k)10its (l)48its

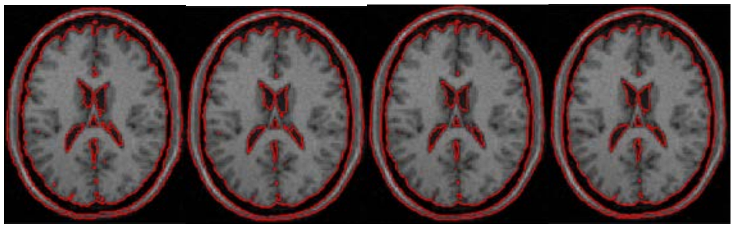

Ours:(m)AI (n) 3its (o) 4its (p) 6 its

Figure 7. Comparation among 4 Methods for Brain-MRI Images. (a), (d), (g) and (j) are the Initial Contours by Manual for various Methods and (m) is the Initial Contour by our Autonomous Method; (c):488 Iterations and 4.97s by CV, (f) :22 Iterations and 1.91s by Bernard, (i): 70 Iterations and 0.47s by SBGFRLS, (l):48 Iterations and 0.51s by ours based on (j), (p): 6 Iterations and 0.26s (include initialization) by ours based on (m), with $\alpha_0 = -1, \lambda_0 = 15$ and $\lambda = 25$. Others are some Middle Results during Evolution. Abbr: IC- Initial Contour; its-iterations; AI-Autonomous Contour

4. Conclusion

In this paper, we first propose a novel region-based autonomous approach to decide the initial contour, which in most cases results in significant improvement for segmenting heterogeneous images. Because the initial autonomous contours can approximate the actual edges of interesting objects well, level set evolution will start from a place close to the genuine edges. The autonomous initialization method not only reduces manual intervention, but also improves the segmentation result of level set obviously.

On the other hand, we also introduce a novel level set model, which is based on subdomain intensities information. We divide the entire image into a contour, contour interior and contour exterior, and utilize spatial intensities information for evolving zero level set. Performance evaluation has been carried out with different difficulty-segmentation images, and our proposed method is demonstrated to be more robust and effective. However, our method may fail to complicated or inwrought multiphase images. In conclusion, our current work merely focused on a single object or simple multiphase image segmentation, and our future work will focus on improving the multiphase level set model for better segmentation by adjusting the method proposed in this paper. How to extend it to be more suitable for texture image is also an important task for us in the near future.

References

[1] C. M. Li, C. Y. Xu, C. F. Gui and M. D. Fox, “Level set evolution without re-initialization: a new variational formulation”, IEEE Conference on Computer Vision and Pattern Recognition, San Diego, USA, **(2005)** June 20-25, pp. 430-436.

[2] C. Y. Xu, A. Yezzi Jr. and J. L. Prince, “On the relationship between parametric and geometric active contours”, Processing of 34th Asilomar Conference on Signals Systems and Computers, Pacific Grove, CA, USA, **(2000)** October 29-November 1, pp. 483-489.

[3] D. Guo and X. Ming, “Color clustering and learning for image segmentation based on neural networks”, IEEE Transactions on Neural Networks, vol. 16, no. 4, **(2005)**, pp. 925-936.

[4] W. Wen, C. He, and M. Li, “Transition region-based active contour model for image segmentation”, Journal of Electronic Imaging, vol. 22, no. 1, **(2013)**, pp. 013021-013021.

[5] J. A. Yezzi, A. Tsai and A. Willsky, "A fully global approach to image segmentation via coupled curve evolution equations", Journal of Visual Communication and Image Representation, vol. 13, no. 1, **(2002)**, pp. 195-216.
[6] K. Zhang, L. Zhang, H. Song and W. Zhou, "Active contours with selective local or global segmentation: A new formulation and level set method, Image and Vision Computing", vol. 28, no. 4, **(2010)**, pp. 668-676.
[7] M. Kass, A. Witkin and D. Terzopoulous, "Snakes: Active contour models", International Journal of Computer Vision, vol. 1, no. 4, **(1988)**, pp. 321-331.
[8] M. Yang, J. Liu and W. Zhang, "Region-based Active Contour with Neighborhood Information for Image Segmentation", JDCTA: International Journal of Digital Content Technology and its Applications, vol. 5, no. 10, **(2011)**, pp. 322-329.
[9] N. Paragios and R. Deriche, "Geodesic active contours and level sets for detection and tracking of moving objects", IEEE Transaction on Pattern Analysis and Machine Intelligence, vol. 22, no. 3, **(2000)**, pp. 1-15.
[10] B. D. Friboulet, P. Thevenaz and M. Unser, "Variational B-Spline Level-Set: A Linear Filtering Approach for Fast Deformable Model Evolution,IEEE Transaction on Image Processing, vol. 18, no. 6, **(2009)**, pp. 1179-1191.
[11] X. Xie, S. Yong Yeo, M. Mirmehdi, I. Sazonov and P. Nithiarasu, "Image Gradient Based Level Set Methods in 2D and 3D", Deformation Models, vol. 7, **(2013)**, pp. 101-120.
[12] S. Lankton and A. Tannenbaum, "Localizing region-based active contours", IEEE Transaction on Image Processing, vol. 17, no. 11, **(2008)**, pp. 2029-2039.
[13] S. C. Zhu and A. Yuille, "Region competition: Unifying snakes, region growing, and bayes/mdl for multiband image segmentation", IEEE Transactions on Pattern Analysis and Machine Intellgence, vol. 18, no. 9, **(1996)**, pp. 884-900.
[14] W. Hao, S. Zheng, C. Guo and X. Yaocheng, "Level set contour extraction based on data-adaptive Gaussian smoother", World Automation Congress (WAC), Puerto Vallarta, Mexico, **(2012)** June 24-28, pp. 11-15.
[15] S. Osher and J. A. Sethian, "Fronts propagating with curvature dependent speed: algorithms based on Hamilton-Jacobi formulation", Journal of Computational Physics, vol. 79, no. 1, **(1988)**, pp. 12-49.
[16] T. Dietenbeck, M. Alessandrini, D. Friboulet and O. Bernard, "CREASEG: a free software for the evaluation of image segmentation algorithms based on level-set", IEEE International Conference On Image Processing, Hong Kong, China, **(2010)** September 26-29, pp. 26-29.
[17] T. Chan and L. Vese, "Active contours without edges", IEEE Transaction on Image Processing, vol. 10, no. 2, **(2001)**, pp. 266-277.
[18] V. Caselles, R. Kimmel and G. Sapiro, "Geodesic active contours", International Journal of Computer Vision, vol. 22, no. 1, **(1997)**, pp. 61-79.
[19] W. Da Chuan, "Region-Based Level Set Model for Image Segmentation", Advanced Materials Research, vol. 616, **(2013)**, pp. 2223-2228.

Authors

Xiaowei He was born in China, in April 1968. He received the B. S degree in Mathematics from Zhejiang Normal University, and the M. S. degree in Computer Application from Zhejiang University, Jinhua,P.R.China in 1992 and Hangzhou in 2000 respectively. Now, he is an associate professor and also a Master Tutor in Computer Software and Theory in Zhejiang Normal University. His research interests include image processing, signal processing and inverse problems. E-mail: jhhxw@zjnu.cn.

Zhuan Song was born in China, in June 1987. She received the B.S. degree in Computer Science and Technology from Xuchang University, Xuchang, P.R.China in 2010. She received the M.S. degree in Computer Software and Theory from Zhejiang Normal University in 2013. Her research interest is the area of Image Processing. E-mail:shmx_624@163.com.

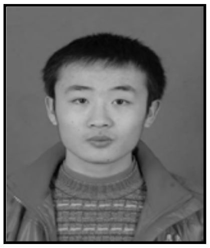

Junli Fan was born in China, in August 1990. He received the B.S. degree in Telecommunication Engineering from Hangzhou Dianzi University in 2012, China. He is currently studying for a M.S. degree in Computer Software and Theory in Zhejiang Normal University. His main research interest is image processing, including image denoising, segmentation and reconstruction .
E-mail:fjl9008@163.com.